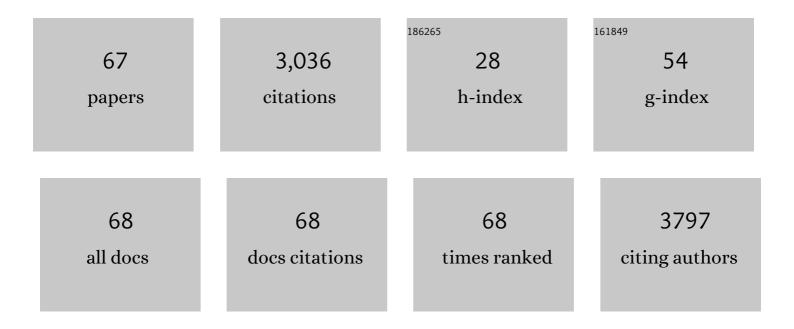
Shingo Matsumoto

List of Publications by Year in descending order

Source: https://exaly.com/author-pdf/7394811/publications.pdf Version: 2024-02-01



| # | Article | IF | CITATIONS |
|----|---|-----|-----------|
| 1 | RF/Microwave Resonators for Preclinical and Clinical EPR Applications: Current Status and Challenges. Applied Magnetic Resonance, 2022, 53, 167-191. | 1.2 | 4 |
| 2 | Hyperpolarized 13 C Magnetic Resonance Imaging of Fumarate Metabolism by Parahydrogenâ€induced Polarization: A Proofâ€of oncept in vivo Study. ChemPhysChem, 2021, 22, 905-905. | 2.1 | 0 |
| 3 | High fidelity triangular sweep of the magnetic field for millisecond scan EPR imaging. Journal of Magnetic Resonance, 2021, 329, 107024. | 2.1 | 8 |
| 4 | Simultaneous T2* mapping of 14N- and 15N-labeled dicarboxy-PROXYLs using CW-EPR-based single-point imaging. Journal of Magnetic Resonance, 2019, 305, 122-130. | 2.1 | 6 |
| 5 | Macrophage derived TNFα promotes hepatic reprogramming to Warburg-like metabolism. Journal of Molecular Medicine, 2019, 97, 1231-1243. | 3.9 | 9 |
| 6 | Proteasome inhibition disrupts the metabolism of fumarate hydratase- deficient tumors by downregulating p62 and c-Myc. Scientific Reports, 2019, 9, 18409. | 3.3 | 10 |
| 7 | Synthesis and evaluation of 13C-labeled 5-5-dimethyl-1-pyrroline-N-oxide aimed at in vivo detection of reactive oxygen species using hyperpolarized 13C-MRI. Free Radical Biology and Medicine, 2019, 131, 18-26. | 2.9 | 9 |
| 8 | Imaging of glucose metabolism by 13C-MRI distinguishes pancreatic cancer subtypes in mice. ELife, 2019, 8, . | 6.0 | 19 |
| 9 | Impact of the Characteristic Impedance of Coaxial Lines on the Sensitivity of a 750-MHz Electronically Tunable EPR Resonator. Applied Magnetic Resonance, 2018, 49, 853-867. | 1.2 | 7 |
| 10 | <scp>EPR</scp> â€based oximetric imaging: a combination of single pointâ€based spatial encoding and <scp>T</scp> ₁ weighting. Magnetic Resonance in Medicine, 2018, 80, 2275-2287. | 3.0 | 12 |
| 11 | Radiotherapy Synergizes with the Hypoxia-Activated Prodrug Evofosfamide: In Vitro and In Vivo Studies. Antioxidants and Redox Signaling, 2018, 28, 131-140. | 5.4 | 27 |
| 12 | Pulsed Electron Paramagnetic Resonance Imaging: Applications in the Studies of Tumor Physiology. Antioxidants and Redox Signaling, 2018, 28, 1378-1393. | 5.4 | 33 |
| 13 | In Vivo Extracellular pH Mapping of Tumors Using Electron Paramagnetic Resonance. Analytical Chemistry, 2018, 90, 13938-13945. | 6.5 | 29 |
| 14 | Long-range heteronuclear J-coupling constants in esters: Implications for 13C metabolic MRI by side-arm parahydrogen-induced polarization. Journal of Magnetic Resonance, 2018, 296, 85-92. | 2.1 | 12 |
| 15 | Metabolic and Physiologic Imaging Biomarkers of the Tumor Microenvironment Predict Treatment Outcome with Radiation or a Hypoxia-Activated Prodrug in Mice. Cancer Research, 2018, 78, 3783-3792. | 0.9 | 42 |
| 16 | Feasibility of in vivo three-dimensional T*2 mapping using dicarboxy-PROXYL and CW-EPR-based single-point imaging. Magnetic Resonance Materials in Physics, Biology, and Medicine, 2017, 30, 291-298. | 2.0 | 13 |
| 17 | Fast backprojection-based reconstruction of spectral-spatial EPR images from projections with the constant sweep of a magnetic field. Journal of Magnetic Resonance, 2017, 281, 44-50. | 2.1 | 19 |
| 18 | Quantitative imaging of pO ₂ in orthotopic murine gliomas: hypoxia correlates with resistance to radiation. Free Radical Research, 2017, 51, 861-871. | 3.3 | 16 |

Shingo Matsumoto

| # | Article | IF | CITATIONS |
|----|--|------|-----------|
| 19 | A 750-MHz electronically tunable resonator using microstrip line couplers for electron paramagnetic resonance imaging of a mouse tumor-bearing leg. IEEE Transactions on Biomedical Engineering, 2017, 65, 1-1. | 4.2 | 5 |
| 20 | Effect of amifostine, a radiation-protecting drug, on oxygen concentration in tissue measured by EPR oximetry and imaging. Journal of Clinical Biochemistry and Nutrition, 2017, 60, 151-155. | 1.4 | 14 |
| 21 | Accelerated 4D quantitative single point EPR imaging using modelâ€based reconstruction. Magnetic Resonance in Medicine, 2015, 73, 1692-1701. | 3.0 | 8 |
| 22 | 13C-MR Spectroscopic Imaging with Hyperpolarized [1-13C]pyruvate Detects Early Response to Radiotherapy in SCC Tumors and HT-29 Tumors. Clinical Cancer Research, 2015, 21, 5073-5081. | 7.0 | 54 |
| 23 | Pyruvate Induces Transient Tumor Hypoxia by Enhancing Mitochondrial Oxygen Consumption and Potentiates the Anti-Tumor Effect of a Hypoxia-Activated Prodrug TH-302. PLoS ONE, 2014, 9, e107995. | 2.5 | 35 |
| 24 | <i>In Vivo</i> Imaging of Tumor Physiological, Metabolic, and Redox Changes in Response to the Anti-Angiogenic Agent Sunitinib: Longitudinal Assessment to Identify Transient Vascular Renormalization. Antioxidants and Redox Signaling, 2014, 21, 1145-1155. | 5.4 | 41 |
| 25 | Targeting ABL1-Mediated Oxidative Stress Adaptation in Fumarate Hydratase-Deficient Cancer. Cancer Cell, 2014, 26, 840-850. | 16.8 | 87 |
| 26 | Artifact suppression in electron paramagnetic resonance imaging of 14 N- and 15 N-labeled nitroxyl radicals with asymmetric absorption spectra. Journal of Magnetic Resonance, 2014, 247, 31-37. | 2.1 | 3 |
| 27 | Magnetic Resonance Imaging of the Tumor Microenvironment in Radiotherapy: Perfusion, Hypoxia, and Metabolism. Seminars in Radiation Oncology, 2014, 24, 210-217. | 2.2 | 61 |
| 28 | Fourâ€channel surface coil array for 300â€MHz pulsed EPR imaging: Proofâ€ofâ€concept experiments. Magnetic Resonance in Medicine, 2014, 71, 853-858. | 3.0 | 8 |
| 29 | EPR oxygen imaging and hyperpolarized ¹³ C MRI of pyruvate metabolism as noninvasive biomarkers of tumor treatment response to a glycolysis inhibitor 3â€bromopyruvate. Magnetic Resonance in Medicine, 2013, 69, 1443-1450. | 3.0 | 44 |
| 30 | Magnetic resonance imaging of tumor oxygenation and metabolic profile. Acta Oncológica, 2013, 52, 1248-1256. | 1.8 | 17 |
| 31 | Single Acquisition Quantitative Singleâ€Point Electron Paramagnetic Resonance Imaging. Magnetic Resonance in Medicine, 2013, 70, 1173-1181. | 3.0 | 18 |
| 32 | Evaluation of partial k-space strategies to speed up time-domain EPR imaging. Magnetic Resonance in Medicine, 2013, 70, 745-753. | 3.0 | 9 |
| 33 | Electron Paramagnetic Resonance Imaging of Tumor pO ₂ . Radiation Research, 2012, 177, 376-386. | 1.5 | 61 |
| 34 | The relationship between tissue oxygenation and redox status using magnetic resonance imaging. International Journal of Oncology, 2012, 41, 2103-2108. | 3.3 | 17 |
| 35 | Transient decrease in tumor oxygenation after intravenous administration of pyruvate. Magnetic Resonance in Medicine, 2012, 67, 801-807. | 3.0 | 24 |
| 36 | Reporting of quantitative oxygen mapping in EPR imaging. Journal of Magnetic Resonance, 2012, 214, 244-251. | 2.1 | 20 |

Shingo Matsumoto

| # | Article | IF | CITATIONS |
|----|--|-----|-----------|
| 37 | Echo-based Single Point Imaging (ESPI): A novel pulsed EPR imaging modality for high spatial resolution and quantitative oximetry. Journal of Magnetic Resonance, 2012, 218, 105-114. | 2.1 | 15 |
| 38 | Longitudinal Imaging Studies of Tumor Microenvironment in Mice Treated with the mTOR Inhibitor Rapamycin. PLoS ONE, 2012, 7, e49456. | 2.5 | 22 |
| 39 | Simultaneous molecular imaging based on electron paramagnetic resonance of 14N- and 15N-labelled nitroxyl radicals. Chemical Communications, 2011, 47, 3245. | 4.1 | 10 |
| 40 | Intracellular Hypoxia of Tumor Tissue Estimated by Noninvasive Electron Paramagnetic Resonance Oximetry Technique Using Paramagnetic Probes. Biological and Pharmaceutical Bulletin, 2011, 34, 142-145. | 1.4 | 24 |
| 41 | Fatty acid amide hydrolase is a key regulator of endocannabinoid-induced myocardial tissue injury. Free Radical Biology and Medicine, 2011, 50, 179-195. | 2.9 | 73 |
| 42 | Magnetic resonance imaging of organic contrast agents in mice: capturing the whole-body redox landscape. Free Radical Biology and Medicine, 2011, 50, 459-468. | 2.9 | 73 |
| 43 | Detecting response of rat C6 glioma tumors to radiotherapy using hyperpolarized [1â€ ¹³ C]pyruvate and ¹³ C magnetic resonance spectroscopic imaging. Magnetic Resonance in Medicine, 2011, 65, 557-563. | 3.0 | 152 |
| 44 | Antiangiogenic Agent Sunitinib Transiently Increases Tumor Oxygenation and Suppresses Cycling Hypoxia. Cancer Research, 2011, 71, 6350-6359. | 0.9 | 120 |
| 45 | Low-Field Magnetic Resonance Imaging to Visualize Chronic and Cycling Hypoxia in Tumor-Bearing Mice. Cancer Research, 2010, 70, 6427-6436. | 0.9 | 120 |
| 46 | Imaging Cycling Tumor Hypoxia. Cancer Research, 2010, 70, 10019-10023. | 0.9 | 183 |
| 47 | Cannabidiol Attenuates Cardiac Dysfunction, Oxidative Stress, Fibrosis, and Inflammatory and Cell Death Signaling Pathways in Diabetic Cardiomyopathy. Journal of the American College of Cardiology, 2010, 56, 2115-2125. | 2.8 | 389 |
| 48 | Simultaneous imaging of tumor oxygenation and microvascular permeability using Overhauser enhanced MRI. Proceedings of the National Academy of Sciences of the United States of America, 2009, 106, 17898-17903. | 7.1 | 87 |
| 49 | Reconstruction for Time-Domain In Vivo EPR 3D Multigradient Oximetric Imaging—A Parallel Processing Perspective. International Journal of Biomedical Imaging, 2009, 2009, 1-12. | 3.9 | 6 |
| 50 | Pulsed EPR imaging of nitroxides in mice. Journal of Magnetic Resonance, 2009, 197, 181-185. | 2.1 | 51 |
| 51 | Half-Life Mapping of Nitroxyl Radicals with Three-Dimensional Electron Paramagnetic Resonance Imaging at an Interval of 3.6 Seconds. Analytical Chemistry, 2009, 81, 7501-7506. | 6.5 | 42 |
| 52 | Dynamic monitoring of localized tumor oxygenation changes using RF pulsed electron paramagnetic resonance in conscious mice. Magnetic Resonance in Medicine, 2008, 59, 619-625. | 3.0 | 18 |
| 53 | Synthesis of Nitroxyl Radicals for Overhauser-enhanced Magnetic Resonance Imaging. Archiv Der Pharmazie, 2008, 341, 548-553. | 4.1 | 23 |
| 54 | Improvement of temporal resolution for three-dimensional continuous-wave electron paramagnetic resonance imaging. Review of Scientific Instruments, 2008, 79, 123701. | 1.3 | 36 |

SHINGO ΜΑΤSUMOTO

| # | Article | IF | CITATIONS |
|----|--|-----|-----------|
| 55 | Low-field paramagnetic resonance imaging of tumor oxygenation and glycolytic activity in mice. Journal of Clinical Investigation, 2008, 118, 1965-73. | 8.2 | 98 |
| 56 | Are Free Radical Reactions Increased in the Diabetic Eye?. Antioxidants and Redox Signaling, 2007, 9, 367-373. | 5.4 | 11 |
| 57 | Advantageous application of a surface coil to EPR irradiation in overhauser-enhanced MRI. Magnetic Resonance in Medicine, 2007, 57, 806-811. | 3.0 | 37 |
| 58 | Use of multi-coil parallel-gap resonators for co-registration EPR/NMR imaging. Journal of Magnetic Resonance, 2007, 184, 29-38. | 2.1 | 36 |
| 59 | Simultaneous molecular imaging of redox reactions monitored by Overhauser-enhanced MRI with 14N- and 15N-labeled nitroxyl radicals. Proceedings of the National Academy of Sciences of the United States of America, 2006, 103, 1463-1468. | 7.1 | 146 |
| 60 | A composite resonator assembly suitable for EPR/NMR coregistration imaging. Concepts in Magnetic Resonance Part B, 2005, 25B, 1-11. | 0.7 | 16 |
| 61 | Influence of protonT1 on oxymetry using Overhauser enhanced magnetic resonance imaging. Magnetic Resonance in Medicine, 2005, 54, 213-217. | 3.0 | 22 |
| 62 | Absolute oxygen tension (pO2) in murine fatty and muscle tissue as determined by EPR. Magnetic Resonance in Medicine, 2005, 54, 1530-1535. | 3.0 | 78 |
| 63 | In vivo imaging of oxidative stress in the kidney of diabetic mice and its normalization by angiotensin II type 1 receptor blocker. Biochemical and Biophysical Research Communications, 2005, 330, 415-422. | 2.1 | 61 |
| 64 | Evidence for contribution of vascular NAD(P)H oxidase to increased oxidative stress in animal models of diabetes and obesity. Free Radical Biology and Medicine, 2004, 37, 115-123. | 2.9 | 163 |
| 65 | In Vivo Measurement of Redox Status in Streptozotocin-Induced Diabetic Rat Using Targeted Nitroxyl Probes. Antioxidants and Redox Signaling, 2004, 6, 605-611. | 5.4 | 19 |
| 66 | Evalution of oxidative stress in diabetic animals by in vivo electron spin resonance measurement—role of protein kinase C. Diabetes Research and Clinical Practice, 2004, 66, S109-S113. | 2.8 | 4 |
| 67 | Confirmation of Superoxide Generation via Xanthine Oxidase in Streptozotocin-induced Diabetic Mice. Free Radical Research, 2003, 37, 767-772. | 3.3 | 99 |